analytical chemistry

Article

pubs.acs.org/ac

Mitochondria-Targeted Reaction-Based Two-Photon Fluorescent Probe for Imaging of Superoxide Anion in Live Cells and in Vivo

Ping Li, Wen Zhang, Kexiang Li, Xiao Liu, Haibin Xiao, Wei Zhang, and Bo Tang*

College of Chemistry, Chemical Engineering and Materials Science, Engineering Research Center of Pesticide and Medicine Intermediate Clean Production, Ministry of Education, Key Laboratory of Molecular and Nano Probes, Ministry of Education, Shandong Normal University, Jinan, Shandong 250014, People's Republic of China

Supporting Information

ABSTRACT: A newly synthesized reaction-based two-photon (TP) fluorescence imaging probe, 9-butyltriphenylphosphoniumacylamino-2,7-dibenzothiazolineflurene (MF-DBZH), composed of a superoxide anion ($O_2^{\bullet-}$) responsive group and a mitochondria-targeted site, has been shown to have high selectivity toward mitochondrial $O_2^{\bullet-}$ fluxes. The fluorescence intensity of MF-DBZH responds proportionally to changes in $O_2^{\bullet-}$ concentrations. Moreover, MF-DBZH was proved to be insensitive toward pH changes and has high photostability. Favorable features of this probe also include convenient cell loading, easy staining of both cells and small animals, and excellent biocompibility. Most importantly, MF-DBZH gives reliable TP fluorescent signal to changes of $O_2^{\bullet-}$ levels in vivo.

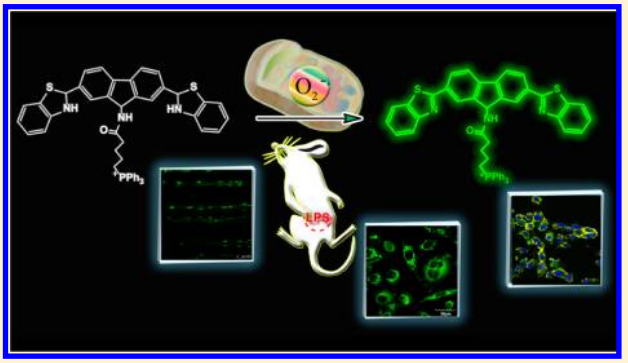

Mitochondria, as the evolutionary relics of aerobic bacteria that invaded the proto-eukaryotic cell, play a crucial role in energy metabolism and apoptosis of aerobic organisms. On the basis of plentiful chemical composition, mitochondria are involved in a wide variety of essential physiological processes. Moreover, studies show that mitochondria are the main intracellular source of reactive oxygen species (ROS), an inevitable side product of normal respiration. ROS are responsible for cell signaling and numerous diseases, including cancer, diabetes, and neurodegenerative disorders.[1,2] Thus, exploring mitochondrial ROS has received extensive attention, especially with the aid of fluorescent imaging techniques due to their high sensitivity and the satisfying spatial and temporal resolution.[3−7] Whether under normal or stress conditions, superoxide anion ($O_2^{\bullet-}$) is first produced within mitochondria, and then rapidly converted to hydrogen peroxide (H_2O_2). Consequentially, they cause the formations of other ROS,[8] which means that $O_2^{\bullet-}$ concentrations may reflect the levels of other ROS. Therefore, to develop a novel fluorescent probe for dynamic and specific tracing mitochondrial $O_2^{\bullet-}$ has become increasingly significant.[5] Furthermore, unraveling the location of $O_2^{\bullet-}$ in subcellular compartments can lead to advances in elucidating its chemistry and biology.

So far, very few examples of ideal small-molecule fluorescent probes have been reported to distinguish $O_2^{\bullet-}$ within mitochondria and in vivo.[9] To accurately detect mitochondrial $O_2^{\bullet-}$ with appropriate selectivity and sensitivity, background perturbation of abundant biomolecules should be inevitably considered, in view of the complicated biological context in mitochondria. Two-photon (TP) excited fluorescence microscopy associated with the probe label is capable of avoiding background fluorescence due to long-wavelength excitation. In particular, two-photon microscopy (TPM) can offer high-resolution, larger depth penetration, as well as less photodamage[10,11] in veridical reporting on biologically active molecules. At present, only a few TP fluorescent probes have been achieved to imaging thiols,[12] H_2O_2,[13] metal ions,[14,15] and so forth; however, TP imaging of $O_2^{\bullet-}$ in mitochondria and in vivo has not been reported until now.

In this work, we sought to construct a new reaction-based TP fluorescent probe (9-butyltriphenylphosphoniumacylamino-2,7-dibenzothiazolineflurene (MF-DBZH)) for imaging $O_2^{\bullet-}$ in mitochondria. This probe consists of a fluorene (a potent TP fluorophore), a $O_2^{\bullet-}$-responsive group, and a mitochondrial-targeted site (Scheme 1). Benzothiazoline was utilized as the receptor owing to its good selectivity toward $O_2^{\bullet-}$.[16] Triphenylphosphonium salt (TPP^+), a well-known potential

Scheme 1. Reaction between MF-DBZH and $O_2^{\bullet-}$

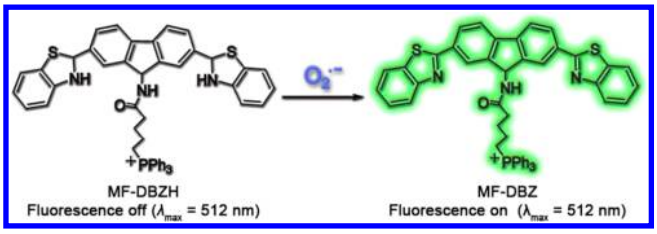

Received: August 1, 2013
Accepted: September 12, 2013
Published: September 12, 2013

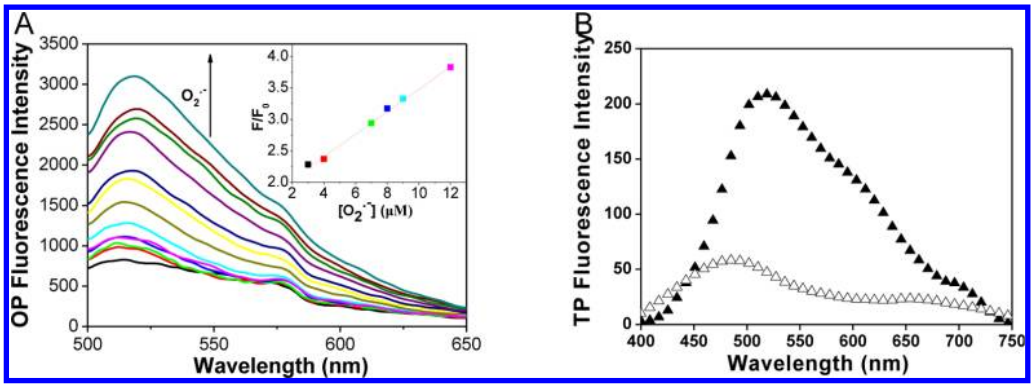

Figure 1. (A) OP fluorescence spectra of MF-DBZH (20 μM) toward various concentrations of $O_2^{\bullet-}$ (0, 0.08, 0.4, 0.6, 0.8, 2.0, 3.0, 4.0, 7.0, 8.0, 9.0, 12 μM, from bottom to top). Inset: the linear relationship between fluorescence ratio (F/F_0) and $O_2^{\bullet-}$ concentrations in the range from 3.0 to 12 μM (probe: 20 μM, Tris−HCl, 10 mM pH 8.0). (B) TP fluorescence spectra for MF-DBZH (20 μM) before (Δ) and after (▲) adding $O_2^{\bullet-}$ (12 μM). All of the spectra were acquired in 10 mM Tris−HCl (pH 8.0) at λex = 483 nm (OP) and λex = 800 nm (TP), respectively.

mitochondria-targeted group,[2,17] was employed to assist MF-DBZH in traversing phospholipid bilayers and accumulating into the mitochondrial matrix driven by the negative membrane potential. We postulated that benzothiazoline dehydrogenation mediated by $O_2^{\bullet-}$ resulted in expanding the conjugated system of the sensor molecule. The above reaction process contributes to the TP fluorescence intensity enhancement of MF-DBZH. Herein, we synthesized and characterized the new TP fluorescent probe, and experimental results demonstrated that it not only could effectively monitor mitochondrial $O_2^{\bullet-}$ but also successfully image the $O_2^{\bullet-}$ fluctuations in mice using intravital TPM.

EXPERIMENTAL SECTION

Materials. 2-Amino-benzenethiol, 4-carboxybutyltriphenylphosphonium bromide (TPP^+), 1-(3-dimethylaminopropyl)-3-ethylcarbodiimide hydrochloride (EDC·HCl), and 1-hydroxybenzotriazole were purchased from Sigma. Probes were prepared by dissolving in dimethyl sulfoxide (DMSO) for further use. The xanthine (XA) solution (1.00 mM) was dissolving in NaOH (1.00×10^{-2} M). The xanthine oxidase (XO) was purchased from Sigma, grade 1: From Buttermilk, and a stock solution of XO (0.5 U/mL) was prepared in 2.30 M $(NH_4)_2SO_4$, 1.00×10^{-2} M sodium salicylate biology buffer, stored at 2−8 °C. L-Glutathione reduced (GSH), *tert*-butyl hydroperoxide (*t*-BuOOH, 70% aqueous solution), hydrogen peroxide (H_2O_2, 30% aqueous solution), sodium hypochlorite (NaOCl, 5% aqueous solution), DMSO, 3-(aminopropyl)-1-hydroxy-3-isopropyl-2-oxo-1-triazene (NOC-5), phorbol 12-myristate 13-acetate (PMA), 3-(4,5-dimethylthiazol-2-yl)-2,5-diphenyltetrazolium bromide (MTT), and Dulbecco's modified Eagle's medium (DMEM) were purchased from Sigma. 4,5-Dihydroxy-1,3-benzenedisulfonic acid disodium salt (Tiron) was purchased from Shanghai Reagent Co. Ltd. (Shanghai, China). All the chemicals used were of analytical−reagent grade, and doubly distilled water was used throughout.

Instrumentation. ^{1}H NMR spectra were determined by 300 MHz using Bruker NMR spectrometers. The mass spectra were obtained by an ABI 4000 MSD. The one-photon excited fluorescence spectra measurements were performed using an FLS-920 Edinburgh fluorescence spectrometer and Cary Eclipse fluorescence spectrophotometer (Supporting Information Figure S-2). Two-photon excited fluorescence spectra were measured using a Tsunami 3941-M3-BB Ti:sapphire femtosecond laser as exciting light source (800 nm) with a pulse width of <150 fs and a repetition rate of 80 MHz, and a USB2000 (bought from Ocean Optics, Inc.) was used as the recorder.

Cell Culture. HepG2 cells and CHO.K1 cells were cultured in DMEM containing 10% fetal bovine serum, 1% penicillin, and 1% streptomycin at 37 °C (w/v) in a 5% CO_2/95% air incubator MCO-15AC (Sanyo, Tokyo, Japan). The concentrations of counted cells were adjusted to 1×10^6 cells mL^{-1} for confocal imaging in high-glucose DMEM (4.5 g of glucose/L) supplemented with 10% fetal bovine serum (FBS), $NaHCO_3$ (2 ng/L), and 1% antibiotics (penicillin/streptomycin, 100 U/mL). Cultures were maintained at 37 °C under a humidified atmosphere containing 5% CO_2.

Cell Extracts. Cell concentration was adjusted to 1×10^6 cells mL^{-1}. Cells with PMA stimulation or without PMA stimulation were suspended in a volume of PBS buffer and disrupted for 10 min in a VC 130PB ultrasonic disintegrator (<4 °C). The broken cell suspension was centrifuged at 4000 rpm for 10 min, and the pellet was discarded. Then the cell extracts were divided into several parts with addition of superoxide dismutase (SOD) (200 U) or Tiron (10 μM), and then MF-DBZH (20 μM) was added.

Mice Culture. Eight-to-ten week old wild-type BalB/C mice (male) were given an ip injection of lipopolysaccharide (LPS) (1 mg in 1 mL of saline). After 4 h, the mice were anesthetized with 4% chloral hydrate (3 mL/kg) by intraperitoneal injection and the abdominal fur was removed. Then, the mice were intraperitoneally injected with MF-DBZH (100 μM). As a control, untreated with LPS only with MF-DBZH (100 μM) were prepared.

Fluorescence Imaging. One-photon confocal fluorescent images were acquired on a Leica TCS SP5 confocal laser-scanning microscope with an objective lens (×40). The excitation wavelengths were 405 nm (5 mW), 488 nm (15 mW), and 514 nm (15 mW), respectively. Cell imaging was carried out after washing cells with Tris−HCl (0.10 M) for three times. The TP imaging of cells were obtained with an Olympus FV1000MPE with a 60× water objective. TP images of mice were captured with a Leica TCS MP5 with a 25× water objective. All the Ti:sapphire laser was used to excite the specimen at 770 nm, and transmissivity was 6%.

MTT Assay. HL-7702 cells (10^6 cell mL^{-1}) were dispersed within replicate 96-well microtiter plates to a total volume of 200 μL $well^{-1}$. Plates were maintained at 37 °C in a 5% CO_2/95% air incubator for 4 h. Then HL-7702 cells were incubated

dx.doi.org/10.1021/ac402409m | *Anal. Chem.* 2013, 85, 9877−9881

for 24 h upon different probe concentrations of 10^{-7}, 10^{-6}, 10^{-5}, 10^{-4}, and 5×10^{-4} M. MTT solution (5 mg mL^{-1}, PBS) was then added to each well. After 4 h, the remaining MTT solution was removed, and 150 μL of DMSO was added to each well to dissolve the formazan crystals. Absorbance was measured at 490 nm in a Triturus microplate reader. Calculation of IC50 values was performed according to Huber and Koella.[18]

RESULTS AND DISCUSSION

Fluorescent Response of MF-DBZH to $O_2^{\bullet-}$. Photophysical aspects of MF-DBZH were studied systematically in simulated physiological conditions (10 mM Tris–HCl buffer, pH 8.0). According to expectation, the presence of $O_2^{\bullet-}$ gave rise to remarkable increase of MF-DBZH fluorescence at the maximum wavelength of 512 nm, excited at 483 nm of one-photon (OP) and 800 nm of TP, respectively (Figure 1, parts A and B). Moreover, the dose-dependent OP fluorescence enhancement of MF-DBZH showed a good linearity with the detection limit of 9.5 nM for $O_2^{\bullet-}$ (Figure 1A inset and Supporting Information Figure S-1). The results revealed that MF-DBZH could measure $O_2^{\bullet-}$ quantitatively. Moreover, the nature of MF-DBZH included instantaneous response to $O_2^{\bullet-}$ and excellent photostability (Supporting Information Figure S-2).

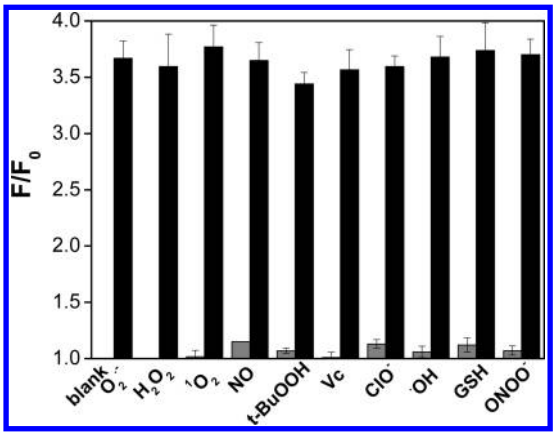

Figure 2. Fluorescence ratio (F/F_0) of MF-DBZH to various reactive species. Gray bars represent the addition of an excess of reactive species (1.2 mM for H_2O_2, GSH; 6 mM for $^1O_2$, NO; 2.4 mM for Vc; 0.6 mM for ClO^-, *t*-BuOOH, ·OH; 0.36 mM for $ONOO^-$). Black bars represent the subsequent addition of 12 μM $O_2^{\bullet-}$ to the solution (MF-DBZH: 20 μM, 10 mM Tris–HCl buffer pH 8.0).

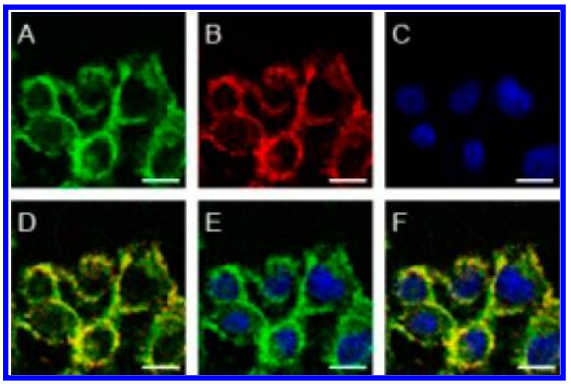

Figure 4. OP microscope images of HepG2 cells with multiple labels. HepG2 cells were stimulated for 1 h with PMA (100 ng/mL) and incubated for 20 min with MF-DBZH (20 μM), Mito-SOX Red (5.0 μM), and Hoechst 33342 (10 μM), simultaneously. Images shown above are signals from (A) MF-DBZH, green; (B) Mito-SOX Red, red; (C) Hoechst 33342, blue; (D) overlay image of panels A and B; (E) overlay image of panels A and C; (F) overlay image of panels A–C. The excitation wavelengths for MF-DBZH, Mito-SOX Red, and Hoechst 33342 were 488, 514, and 405 nm, individually. The corresponding emissions were collected at 490–550 nm (MF-DBZH), 570–610 nm (Mito-SOX Red), and 410–480 nm (Hoechst 33342). Scale bar = 15 μm.

Selectivity of MF-DBZH toward $O_2^{\bullet-}$. In order to inspect whether MF-DBZH could specifically monitor $O_2^{\bullet-}$ under complicated intracellular and mitochondrial environment, we tested its ability to discriminate between $O_2^{\bullet-}$ and various bioanalytes, such as competing ROS, RNS, and relevant biological substances. As shown in Figure 2, MF-DBZH did not display evident fluorescence increase at the present of other ROS or relevant substances, including hydrogen peroxide (H_2O_2), singlet oxygen ($^1O_2$), nitric oxide (NO), TBHP, hypochlorite (OCl^-), hydroxyl radical (·OH), peroxynitrite ($ONOO^-$), glutathione (GSH), and ascorbic acid (Vc). Nevertheless, after $O_2^{\bullet-}$ was added into the above-mentioned analytical system, the obvious increase of MF-DBZH fluorescence intensity is witnessed. Thus, these results strongly suggested MF-DBZH was highly selective for $O_2^{\bullet-}$. Besides, there was negligible fluorescence responses of MF-DBZH within the physiological pH (Supporting Information Figure S-3), which means pH changes did not influence the detection of $O_2^{\bullet-}$.

Visualizing Intracellular Endogenous $O_2^{\bullet-}$ by TP Fluorescent Microscopy. Then, we tested whether MF-DBZH could selectively detect endogenous $O_2^{\bullet-}$ in live cells.

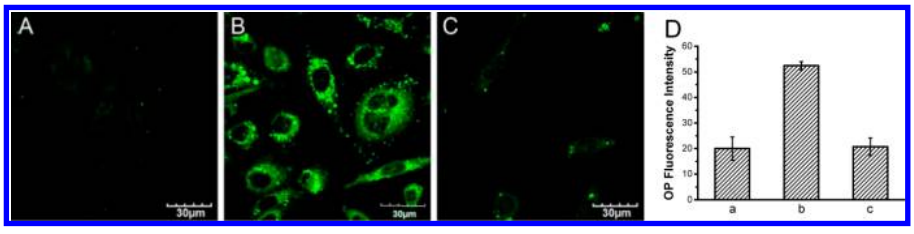

Figure 3. TP microscope images of live HepG2 cells. (A) HepG2 cells incubated with MF-DBZH (20 μM) for 20 min. (B) Cells stimulated with PMA (100 ng/mL) for 1 h, and then incubated with MF-DBZH (20 μM) for 20 min. (C) Cells stimulated with PMA (100 ng/mL) for 1 h, then treated with Tiron (100 μM) for 30 min, and then incubated with MF-DBZH (20 μM) for 20 min. All cells were rinsed three times with 0.1 M Tris–HCl buffer before imaging. Images were collected in optical windows between 500 and 550 nm upon excitation at 770 nm for MF-DBZH. Scale bar = 30 μm. (D) Relative OP fluorescent intensity of MF-DBZH-labeled cells in panels A–C. Cells shown are representative images from replicate experiments (n = 5).

dx.doi.org/10.1021/ac402409m | *Anal. Chem.* 2013, 85, 9877–9881

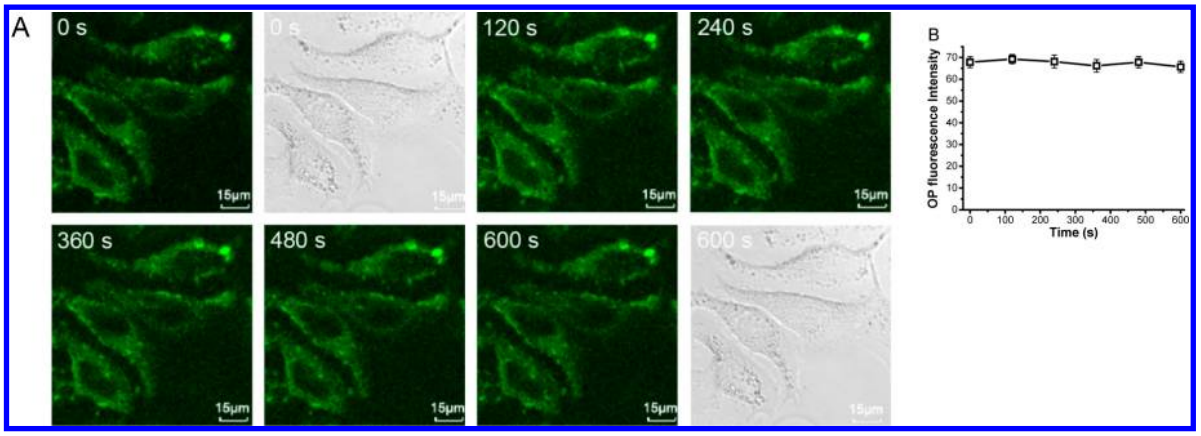

Figure 5. Test of MF-DBZH photostability. (A) HeLa cells were treated with PMA (100 ng/mL) for 1 h, and then incubated with MF-DBZH for 20 min. HeLa cells were rinsed three times with 0.1 M Tris−HCl buffer before imaging. Scale bar = 15 μm. (B) Relative OP fluorescent intensity of MF-DBZH-labeled cells in panels A−C. Cells shown are representative images from replicate experiments (n = 5).

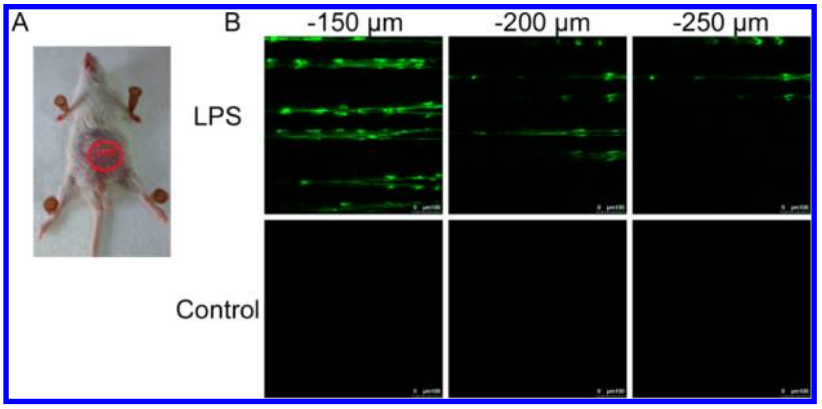

Figure 6. TP microscopy images of the mice with LPS-mediated abdomen injury. (A) $O_2^{\bullet-}$ was produced inside the peritoneal cavity of the mice during the LPS-mediated inflammatory response. (B) TP fluorescent in situ images of mice abdomen incubated with MF-DBZH (100 μM). Images were acquired using 770 nm TP excitation. TP fluorescent emission windows: 500−550 nm. Scale bar = 100 μm.

Cultured HepG2 cells loaded with MF-DBZH were treated to generate excessive $O_2^{\bullet-}$ because of the respiratory burst induced by PMA.[19] As respected, the bright TP fluorescence images were distinctly observed in response to the stimulation (Figure 3B). To further verify selectivity of MF-DBZH for intracellular $O_2^{\bullet-}$, after PMA stimulation, these cells were treated with a Tiron solution (a cell-permeable $O_2^{\bullet-}$ scavenger).[20] TP fluorescence intensity decreased greatly in the processed cells (Figure 3C), which was consistent with interference experiments results. The scavenging $O_2^{\bullet-}$ experiments in cellular extracts demonstrated identical scavenging effects using Tiron or SOD as the scavenger (Supporting Information Figure S-4). In addition, identical visualization results were obtained in CHO.K1 cell lines by OP fluorescent imaging (Supporting Information Figure S-5). These results strongly suggested MF-DBZH was able to monitor the changes of intracellular $O_2^{\bullet-}$ levels with high sensitivity and selectivity.

Co-Staining Imaging with MF-DBZH and Mito-SOX Red in Live Cells. We then evaluated mitochondria-targeted ability of the candidate probe, since it offers considerable sensitivity and selectivity for intracellular $O_2^{\bullet-}$. Simultaneous staining was performed in HepG2 cells, using MF-DBZH (green channel, Figure 4A), Mito-SOX Red (a commercially available mitochondria-specific dye, red channel, Figure 4B), and Hoechst 33342 (a well-known commercial nuclear dye, blue channel, Figure 4C). In merged OP fluorescence images, fluorescence of MF-DBZH and Mito-SOX Red (Figure 4, parts D and F) extensively overlapped compared with the merged image of MF-DBZH and Hoechst 33342 (Figure 4E). The colocalization coefficient of the fluorescent intensity distribution between the green and red channels was 0.89.[21] These results confirmed that MF-DBZH could localize reliably to the mitochondria and respond toward rises in mitochondrial $O_2^{\bullet-}$.

Photostability Evaluation of MF-DBZH in Live Cells. The photostability of MF-DBZH had been investigated in live cells shown in Figure 5. Fluorescent intensity did not show any apparent changes in these cells, suggesting that the probe leakage did not occur during experimentation. Besides, MF-DBZH was verified to have low cytotoxicity and no photobleaching (Figure 5 and Supporting Information Figure S-6), which greatly facilitates protracted fluorescence observations of live cells. All this evidence clearly showed MF-DBZH could faithfully indicate changes of intracellular $O_2^{\bullet-}$.

Imaging $O_2^{\bullet-}$ in Mice by TP Fluorescent Microscopy. To further validate application for biological imaging, MF-DBZH was used to track $O_2^{\bullet-}$ fluctuations in vivo (Figure 6). TP fluorescence images were acquired in the mouse with severe abdomen injury induced by LPS.[22] Notably, Figure 6B shows clearly that MF-DBZH in the LPS-treated mouse abdomen fluoresced quite strongly, in contrast to the control group without LPS treatment. The fluorescent brightness difference can be represented as $O_2^{\bullet-}$ distribution profiles. Imaging results

dx.doi.org/10.1021/ac402409m | Anal. Chem. 2013, 85, 9877−9881

indicated the relationship between excessively produced $O_2^{\bullet-}$ and inflammation. Moreover, these images were obtained at the depths of 150−250 μm, which obviously displayed TP advantages in tissue penetration depth. These results provide direct evidence that MF-DBZH is a useful tool for visualizing $O_2^{\bullet-}$ fluxes in vivo.

CONCLUSIONS

In summary, a new reaction-based TP fluorescence probe, MF-DBZH, has been developed to imaging $O_2^{\bullet-}$ with high selectivity and sensitivity. MF-DBZH possesses distinct advantages, including pH-insensitivity, high photostability, convenient staining of both cells and mice, and excellent biocompibility. More importantly, this probe can preferably accumulate in mitochondria and successfully follow $O_2^{\bullet-}$ fluctuations in vivo by TP fluorescence imaging. Taken altogether, MF-DBZH with TPM fluorescence imaging is an extremely promising approach for monitoring $O_2^{\bullet-}$ changes in various biological contexts.

ASSOCIATED CONTENT

Supporting Information

Synthesis, characterization, and experimental details. This material is available free of charge via the Internet at http://pubs.acs.org.

AUTHOR INFORMATION

Corresponding Author

*E-mail: tangb@sdnu.edu.cn. Fax: 86 531-86180017.

Notes

The authors declare no competing financial interest.

ACKNOWLEDGMENTS

This work was supported by the 973 Program (2013CB933800), the National Natural Science Foundation of China (21227005, 21035003, and 21205073), the Specialized Research Fund for the Doctoral Program of Higher Education of China (20113704130001), and the Program for Changjiang Scholars and Innovative Research Team in University and Science and Technology Development Programs of Shandong Province of China (2010G0020243). The authors thank Professor Xiaoqiang Yu for two-photon imaging and Professor Jie Pan for support with mice model.

REFERENCES

(1) Wallace, D. C. *Science* **1999**, *283*, 1482−1488.
(2) Yousif, L. F.; Stewart, K. M.; Kelley, S. O. *ChemBioChem* **2009**, *10*, 1939−1950.
(3) Koide, Y.; Urano, Y.; Kenmoku, S.; Kojima, H.; Nagano, T. *J. Am. Chem. Soc.* **2007**, *129*, 10324−10325.
(4) Dickinson, B. C.; Chang, C. J. *J. Am. Chem. Soc.* **2008**, *130*, 9638−9639.
(5) Wang, W.; Fang, H.; Groom, L.; Cheng, A.; Zhang, W.; Liu, J.; Wang, X.; Li, K.; Han, P.; Zheng, M.; Yin, J.; Wang, W.; Mattson, M. P.; Kao, J. P.; Lakatta, E. G.; Sheu, S. S.; Ouyang, K.; Chen, J.; Dirksen, R. T.; Cheng, H. *Cell* **2008**, *134*, 279−290.
(6) Dodani, S. C.; Leary, S. C.; Cobine, P. A.; Winge, D. R.; Chang, C. J. *J. Am. Chem. Soc.* **2011**, *133*, 8606−8616.
(7) Masanta, G.; Lim, C. S.; Kim, H. J.; Han, J. H.; Kim, H. M.; Cho, B. R. *J. Am. Chem. Soc.* **2011**, *133*, 5698−5700.
(8) Turrens, J. F. *J. Physiol.* **2003**, *552*, 335−344.
(9) Robinson, K. M.; Janes, M. S.; Pehar, M.; Monette, J. S.; Ross, M. F.; Hagen, T. M.; Murphy, M. P.; Beckman, J. S. *Proc. Natl. Acad. Sci. U.S.A.* **2006**, *103*, 15038−15043.
(10) Denk, W.; Strickler, J. H.; Webb, W. W. *Science* **1990**, *248*, 73−76.
(11) Kim, H. M.; An, M. J.; Hong, J. H.; Jeong, B. H.; Kwon, O.; Hyon, J.-Y.; Hong, S.-C.; Lee, K. J.; Cho, B. R. *Angew. Chem.* **2008**, *120*, 2263−2266.
(12) Lee, J. H.; Lim, C. S.; Tian, Y. S.; Han, J. H.; Cho, B. R. *J. Am. Chem. Soc.* **2010**, *132*, 1216−1217.
(13) Chung, C.; Srikun, D.; Lim, C. S.; Chang, C. J.; Cho, B. R. *Chem. Commun.* **2011**, *47*, 9618−9620.
(14) Kim, M. K.; Lim, C. S.; Hong, J. T.; Han, J. H.; Jang, H. Y.; Kim, H. M.; Cho, B. R. *Angew. Chem.* **2010**, *122*, 374−377.
(15) Kim, H. J.; Han, J. H.; Kim, M. K.; Lim, C. S.; Kim, H. M.; Cho, B. R. *Angew. Chem.* **2010**, *122*, 6938−6941.
(16) Li, H.; Li, Q.; Wang, X.; Xu, K.; Chen, Z.; Gong, X.; Liu, X.; Tong, L.; Tang, B. *Anal. Chem.* **2009**, *81*, 2193−2198.
(17) Murphy, M. P.; Smith, R. A. *Annu. Rev. Pharmacol. Toxicol.* **2007**, *47*, 629.
(18) Huber, W.; Koella, J. C. *Acta Trop.* **1993**, *55*, 257−261.
(19) Tyagi, S. R.; Tamura, M.; Burnham, D. N.; Lambeth, J. D. *J. Biol. Chem.* **1988**, *263*, 13191−13198.
(20) Xu, K.; Liu, X.; Tang, B.; Yang, G.; Yang, Y.; An, L. *Chem.—Eur. J.* **2007**, *13*, 1411−1416.
(21) Mannders, E. M. M.; Stap, J.; Brakenhoff, G. J.; Driel, R. V.; Aten, J. A. *J. Cell Sci.* **1992**, *103*, 857−863.
(22) Lee, D.; Khaja, S.; Velasquez-Castano, J. C.; Dasari, M.; Sun, C.; Petros, J.; Taylor, W. R.; Murthy, N. *Nat. Mater.* **2007**, *6*, 765−769.